ACI MATERIALS JOURNAL TECHNICAL PAPER

Title no. 110-M39

Characterizing Cracking Potential of Cementitious Mixtures Based on Shrinkage and Humidity Drop Rate

by Ya Wei and Will Hansen

*Tensile stress develops as early as upon final setting in concrete if shrinkage deformation due to thermal or hygral changes is restrained either externally or internally. Quantifying such stress and the associated cracking potential in concrete members is a difficult task due to many factors involved, such as creep and stress relaxation, tensile strength development, and the combined thermal and hygral effects. In this study, the early-age tensile stress development and cracking potential were investigated on cement paste and concrete with and without slag cement for different water-cementitious material ratios (*w/cm*). A method is proposed for evaluating early-age cracking potential based on experimental results and numerical simulations. It was found that cracking potential is closely related to the shrinkage rate rather than the shrinkage magnitude, confirming the findings of other studies. A unique relationship was found to exist between the shrinkage rate and cracking time for the cement paste studied. The cracking time was expressed as a function of the relative humidity (RH) drop rate and the aggregate content of a concrete mixture based on a relationship between mixture shrinkage and RH established previously. It was found that a high RH drop rate increases cracking potential. Concrete containing an aggregate content of 50% or less is highly sensitive to cracking, and thus is crucial for the cracking potential of the outer layer of concrete exposed to the environment without appropriate curing. This study proposes a new methodology for evaluating cracking potential, which has implications for mitigating early-age cracking in concrete members.*

Keywords: aggregate content; concrete relative humidity; cracking potential; restrained shrinkage stress; RH drop rate; shrinkage rate.

INTRODUCTION

Shrinkage cracking commonly occurs in concrete structures and is a big concern with regard to service life and appearance. Concrete structures experience volume changes as a result of thermal- and moisture-related deformations during hardening and drying. Tensile stresses develop quickly if shrinkage deformations are restrained. This can lead to cracking and associated durability problems.

Several test methods have been proposed to assess the cracking potential of concrete,[1,2] including tests using restrained ring specimens[2-4] and tests using restrained linear specimens.[5-9] The cracking potential of concrete has been classified according to time-to-cracking and stress rates obtained from the restrained ring test with specimens exposed to external drying.[10,11] The four classes are[12]: high cracking potential with tensile stress rates exceeding 0.34 MPa/day (50 psi/day), moderate-to-high cracking potential with tensile stress rates between 0.17 MPa/day (25 psi/day) and 0.34 MPa/day (50 psi/day), moderate-to-low cracking potential with stress rates between 0.10 MPa/day (15 psi/day) and 0.17 MPa/day (25 psi/day), and low cracking potential with stress rates lower than 0.10 MPa/day (15 psi/day).

Quantifying shrinkage-induced stress and assessing associated cracking potential in concrete members have been difficult tasks due to many factors involved, such as creep and stress relaxation, tensile strength and elastic modulus development, and combined thermal and hygral effects. Analyzing the risk of cracking at early ages favors the use of simple methods. In this study, a new methodology is proposed for evaluating the cracking potential of concrete. This methodology uses the concrete shrinkage rate or relative humidity (RH) drop rate as the controlling factor to assess the cracking potential. A critical shrinkage rate at the time of cracking is obtained from experimental measurements on free and restrained specimens. A humidity-shrinkage relationship is used to calculate the critical RH drop-rate values within the concrete as a means for assessing cracking potential. A servo-hydraulic test frame with deformation control from the start of concrete placement is used for tensile stress and cracking behavior evaluations for cement paste and concrete under restraint conditions starting at very early ages.

RESEARCH SIGNIFICANCE

Difficulties in making strain and stress measurements complicate the assessment of cracking potential in concrete members. In this study, a method is proposed based on experimental measurements on linear specimens and analytical simulations for assessing the cracking potential of concrete members subject to constant restraint. This method uses the concrete shrinkage rate or humidity drop rate as the major parameter for characterizing cracking potential. The results of this study are of significance for evaluating and mitigating early-age cracking in concrete members.

EXPERIMENTAL INVESTIGATION

Materials and mixture proportions

Type I ordinary portland cement (OPC) was used. As a supplementary cementitious material, slag cement was used to evaluate its effect on early-age stress development and cracking behavior. The slag cement was Grade 120, and the replacement levels were 30 and 50% of the total cementitious materials by mass. The coarse aggregate was crushed limestone with a maximum size of 12.5 mm (0.5 in). The fine aggregate was natural sand with a fineness modulus of 2.56.

The mixture proportions of the cement pastes and concretes used in this study are presented in Table 1. The cement paste was mixed in a pan mixer. For blended systems, the slag

ACI Materials Journal, V. 110, No. 4, July-August 2013.

ACI member **Ya Wei** *is a Lecturer in the Department of Civil Engineering at Tsinghua University, Beijing, China. She received her PhD from the University of Michigan, Ann Arbor, MI. Her research interests include development and characterization of cementitious composites, pavements design, and performance analysis.*

Will Hansen, *FACI, is a Professor in the Department of Civil and Environmental Engineering at the University of Michigan. His research interests include blended cements, concrete testing, curling and warping of slabs-on-ground, durability, and pavement performance.*

cement was first dry-mixed with OPC for several minutes to achieve a uniform distribution of the solid ingredients. Water was then added to the dry ingredients and mixed for another 3 minutes. The amount of high-range water-reducing admixture was adjusted to achieve adequate workability in low water-cement ratio (*w*/*c*) concrete (*w*/*c* = 0.35).

UNRESTRAINED AND RESTRAINED SHRINKAGE TEST

Unrestrained and restrained shrinkage tests were conducted for measuring free strain and restrained stress developments in the cementitious mixtures. In unrestrained tests, one-dimensional (1-D) linear autogenous shrinkage was measured on sealed specimens by wrapping two layers of plastic sheets around the specimens using a double-walled, water-cooled, stainless steel apparatus. Low specimen-to-mold friction was achieved by placing a soft foam layer on the three contact surfaces. A detailed testing procedure can be found elsewhere.[13]

The restrained tests measured stress development in the cementitious mixtures starting immediately after casting using a horizontal testing frame built for this purpose (as shown in Fig. 1). A linear measurement system, according to Weiss and Shah,[2] has the advantage of relatively straightforward data interpretation. The frame used in this study includes a load cell and an actuator with servo-hydraulic control. To provide sufficient restraint and to avoid drift over a long period of time, the actuator position was controlled so that the concrete can be assumed to be under a "full restraint" condition.[14] This type of frame is known as an

Table 1—Mixture proportions of cement paste and concrete

Mixture	Cement, kg/m^3 (lb/yd^3)	Slag cement, kg/m^3 (lb/yd^3)	Water, kg/m^3 (lb/yd^3)	Coarse aggregate, kg/m^3 (lb/yd^3)	Sand, kg/m^3 (lb/yd^3)	High-range water-reducing admixture, kg/m^3 (lb/yd^3)	*w*/*cm*	Time to cracking, days
P35O	1500 (2528)	—	525 (885)	—	—	—	0.35	0.67
P35G30	1037 (1748)	444 (748)	518 (874)	—	—	—		0.68
C35O	510 (860)	—	178 (300)	387 (652)	1100 (1854)	2.1 (3.5)		*
C35G30	357 (602)	153 (258)	178 (300)	387 (652)	1100 (1854)	2.1 (3.5)		*
P40O	1395 (2351)	—	558 (941)	—	—	—	0.4	0.83
P40G30	964 (1625)	413 (696)	551 (928)	—	—	—		1.5
P40G50	685 (1154)	685 (1154)	548 (924)	—	—	—		5.25
P45O	1303 (2196)	—	586 (988)	—	—	—	0.45	1.9
P45G30	898 (1514)	385 (649)	577 (973)	—	—	—		6.08

*No cracking during time of testing (12 days).

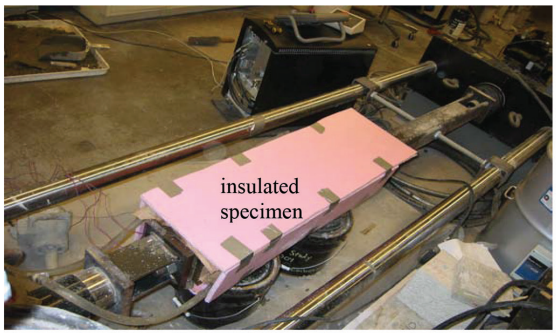

(a) Photo of restrained shrinkage test setup

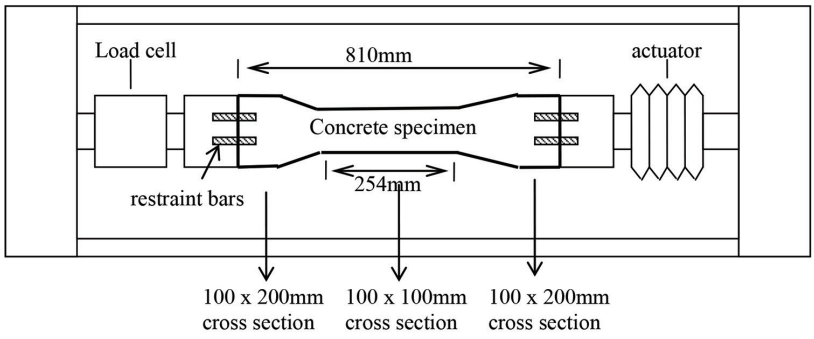

(b) Sketch of top view of the setup (1mm=0.0394in)

Fig. 1—Restrained linear shrinkage test.

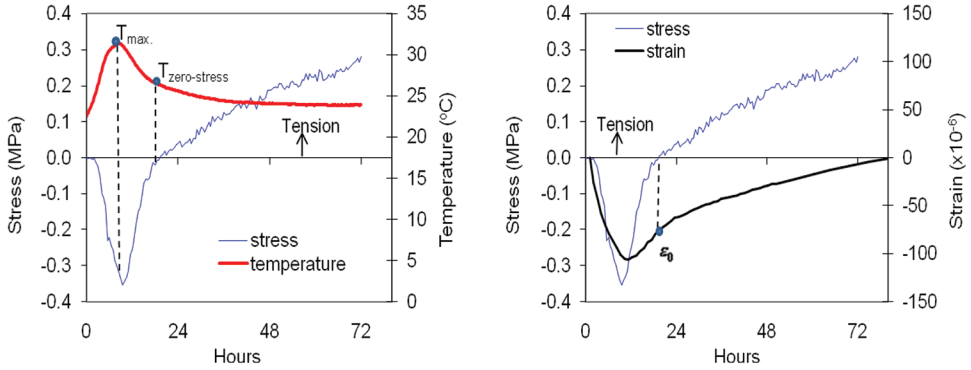

Fig. 2—Typical temperature, total strain, and stress developments of sealed-cured concrete. (Note: 1 MPa = 145 psi; °C = (°F – 32)/1.8.)

active restraining rig for achieving a "full restraint" condition, which is independent of the restraining rigidity of the testing rig.[14-16] The 810 mm (31.9 in.) long specimen was cast directly into a foam-insulated mold held by the frame. Two ends of the specimen were enlarged and the central part has a cross section of 100 x 100 mm (3.9 x 3.9 in.). One end of the specimen was fixed to the load cell and the other end was connected to the actuator by restraint bars that are embedded in the specimen. A thin vinyl sheet was placed between the specimen and the mold to reduce frictional resistance. Immediately after casting, the upper surface of the specimen was covered with a plastic sheet to prevent evaporation. The mold was equipped with copper pipes to circulate constant-temperature (23 ± 1°C [73.4 ± 1.8°F]) water from a heating-cooling control bath. During the entire testing, the specimen was cured under the sealed condition. The temperature distribution in the specimen was measured at three locations along the specimen depth. It was found that the specimens had a uniform temperature distribution at all times. The measurement started immediately after casting. Load was measured during the test and the data were recorded once per minute.

RESULTS AND DISCUSSIONS

Tensile stress development and cracking behavior under constantly restrained conditions

Traditionally, stress development has to be known to assess cracking potential in cementitious mixtures. For a restrained and sealed-cured specimen, the development of early-age stress is a result of thermal and autogenous deformations. The induced stress can be written as $\sigma = (\Delta T \cdot \alpha + \varepsilon_{au}) \cdot E_{eff}$, where ΔT is temperature change with respect to the temperature at final set; α is the coefficient of thermal expansion; ε_{au} is autogenous shrinkage; and E_{eff} is the effective elastic modulus incorporating relaxation effects.

For illustration, Fig. 2 shows typical curves of temperature, strain, and stress developments measured on a sealed-cured concrete specimen. It was found that the restrained stress is induced a few hours after casting. The thermal effect dominates compressive stress development at the start of the test. The temperature increases from the mixing temperature to the maximum due to the heat of cement hydration, and then stabilizes at the end of the first day, indicating no additional contributions to stress development from thermal effects. In Fig. 2(a), $T_{zero\text{-}stress}$ is the temperature when the induced stress switches from compression to tension. After $T_{zero\text{-}stress}$, any temperature drop or autogenous shrinkage, if restrained, will generate tensile stress: $\sigma_{tensile} = ((T - T_{zero\text{-}stress}) \cdot \alpha + (\varepsilon_{au} - \varepsilon_0)) E_{eff}$, where ε_0 is the autogenous shrinkage when the restraint stress switches from compression to tension. ε_0 will be used as the starting point of shrinkage for the purpose of tensile stress evaluation. It should be noted that ε_0 is not necessary to be zero, because the high relaxation property of young concrete causes most of the compressive stress to be relaxed and a rapid change in stress from compression to tension. In this study, shrinkage and the associated tensile stress development after $T_{zero\text{-}stress}$ were reported for paste and concrete mixtures with and without slag cement at *w/c* of 0.35, 0.4, and 0.45 (refer to Table 1). The results are shown in Fig. 3 through 7.

From Fig. 3 through 7, it is seen that cement paste shows much faster development of both free shrinkage and restrained tensile stress as compared with that of concrete. All paste specimens cracked within the first week. The time to cracking of each paste specimen was listed in Table 1. Low water-cementitious material ratio (*w/cm*) pastes show faster shrinkage development, earlier cracking time, and higher strength at cracking. At the same *w/cm*, pastes containing slag cement, especially with a slag cement content of 50%, show delayed cracking time and a slightly higher cracking strength. This might be a result of dilution effect from slag cement that the actual portland cement content is reduced in the blended system, leading to slower autogenous shrinkage and stress development at an early age when cement hydration is not intensive.[13] This effect diminishes at the lower slag cement content (30%). For all concrete mixtures, no cracking was observed during the testing period of 12 days. Compared with cement paste, autogenous shrinkage of concrete is lower and develops more slowly, which allows more time for tensile stress to be relaxed. The concrete containing 30% slag cement behaved similarly to the concrete with OPC only.

New methodology for assessing cracking potential

The traditional method for assessing cracking potential in cementitious mixtures requires stress measurements or calculations under restrained conditions. However, both stress measurement and calculation are difficult to conduct in field structures due to many factors involved. Establishing a practical method for evaluating cracking potential is needed.

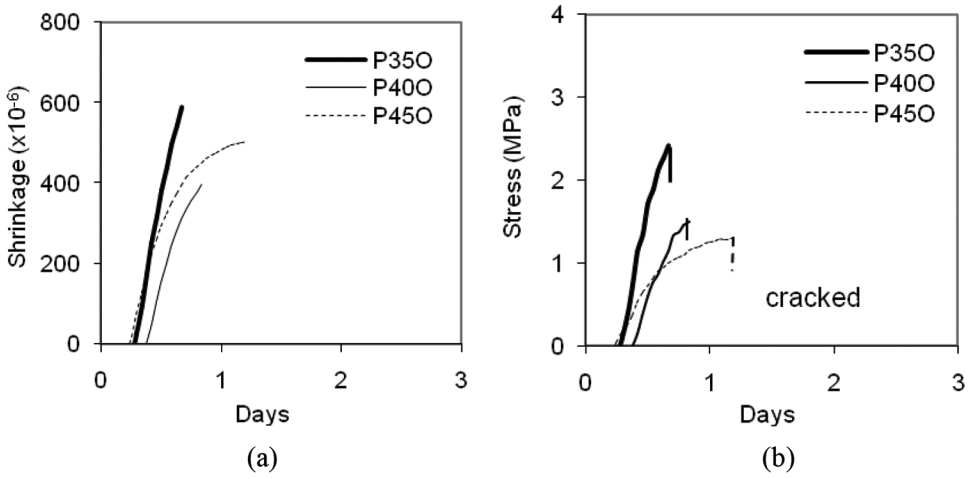

Fig. 3—Unrestrained shrinkage and stress development in fully restrained sealed-cured OPC pastes at w/c *of 0.35, 0.4, and 0.45. (Note: 1 MPa = 145 psi.)*

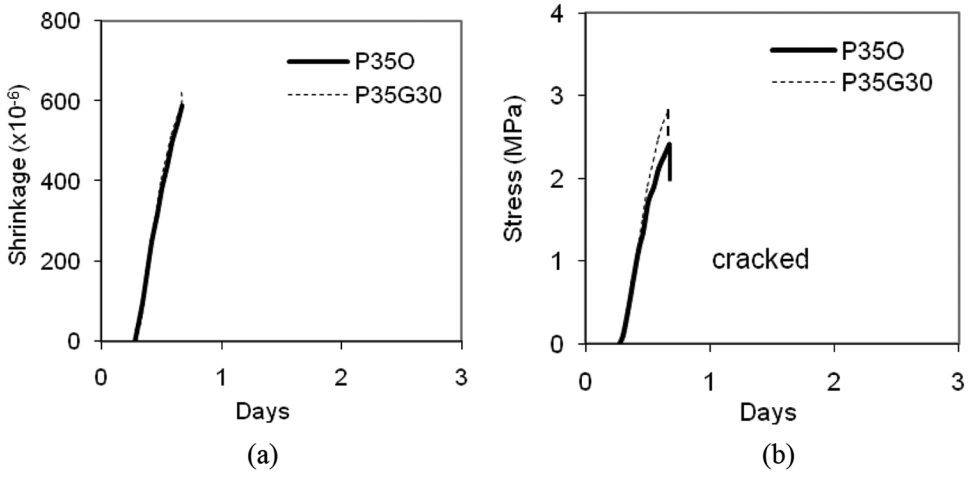

Fig. 4—Unrestrained shrinkage and stress development in fully restrained sealed-cured pastes at w/cm *of 0.35. (Note: 1 MPa = 145 psi.)*

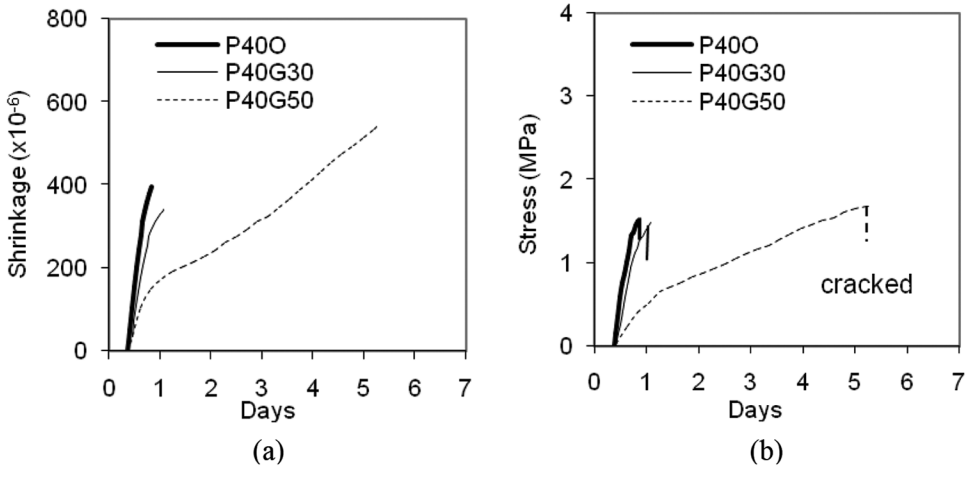

Fig. 5—Unrestrained shrinkage and stress development in fully restrained sealed-cured pastes at w/cm *of 0.4. (Note: 1 MPa = 145 psi.)*

One important observation from the aforementioned experimental results is that the development of tensile stress in a restrained specimen closely follows the free autogenous shrinkage development in a companion specimen, and a higher shrinkage rate causes earlier cracking. This observation is consistent with previous studies.[9,16,17] Therefore, it is worthwhile to investigate the relationship between shrinkage rate ($\dot{\varepsilon}$ in microstrain/h) and the cracking time (t_{cr} in days). The shrinkage rate was calculated based on the measured shrinkage data of cement paste and concrete as

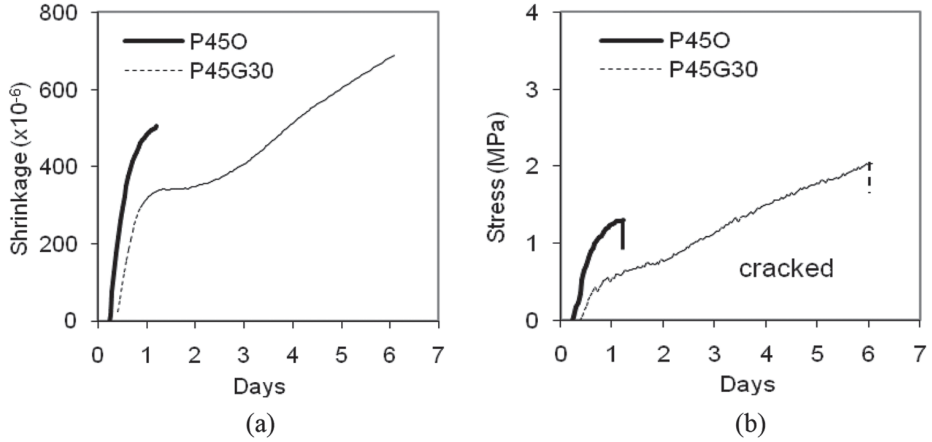

Fig. 6—Unrestrained shrinkage and stress development in fully restrained sealed-cured pastes at w/cm *of 0.45. (Note: 1 MPa = 145 psi.)*

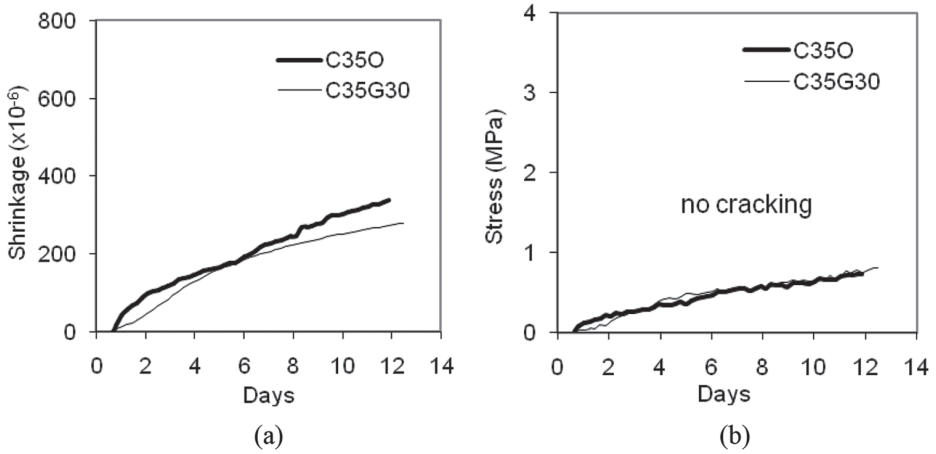

Fig. 7—Unrestrained shrinkage and stress development in fully restrained sealed-cured concretes at w/cm *of 0.35. (Note: 1 MPa = 145 psi.)*

$$\dot{\varepsilon} = \frac{\varepsilon(t+1) - \varepsilon(t)}{\Delta t}$$

in which Δt = 1 hour. The calculated results are shown in Fig. 8, which shows the shrinkage rate at cracking for paste specimens and the shrinkage rate of uncracked concrete specimens. It can be seen that the cracking time t_{cr} for paste specimens is related uniquely to the shrinkage rate at cracking, or critical shrinkage rate $\dot{\varepsilon}_{cr}$, regardless of *w/cm* and presence of slag cement. A best-fit equation can be used to describe this relationship

$$\dot{\varepsilon}_{cr} = \left(\frac{d\varepsilon}{dt}\right)_{cr} = 14\left(t_{cr}/24 - 0.1\right)^{-0.87} \quad (1)$$

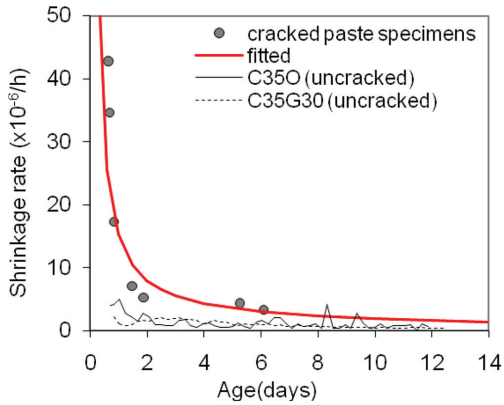

Fig. 8—Shrinkage rate of paste specimens at cracking and measured shrinkage rate of uncracked concrete.

This equation is plotted in Fig. 8 and denoted as "fitted." It is seen that the shrinkage rate at cracking $\dot{\varepsilon}_{cr}$ is inversely related to the time at cracking t_{cr}; the smaller the critical shrinkage rate at a given time, the higher the cracking tendency of the cementitious mixture. A relationship similar to Eq. (1) but in terms of stress rate from ring test measurements has been observed previously by See et al.[17] It forms the basis for the cracking potential classification in the ASTM C1581/C1581M[12] test method.

Because the paste phase rather than the aggregate phase is the source of shrinkage and, consequently, the cause of cracking in concrete, it is reasonable to assume that Eq. (1), established based on paste measurements, also applies to concrete mixtures. The shrinkage rate $\dot{\varepsilon}$ curves of the two

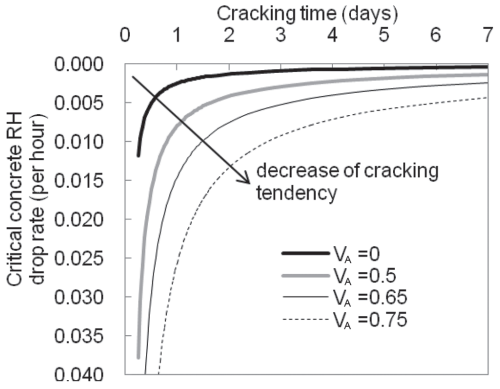

Fig. 9—Calculated critical concrete RH drop rate for concrete with V_A *= 0, 0.5, 0.65, and 0.75 when cracking occurs.*

uncracked concrete mixtures are plotted in Fig. 8. These two curves are below the critical shrinkage rate curve obtained from cracked paste specimens, indicating no cracking would be expected in concrete, which is consistent with the experimental results.

Because the reduction of RH due to self-desiccation in a cementitious mixture is the driving force for autogenous shrinkage,[18] it is possible to use the concrete RH drop rate instead of the shrinkage rate as a parameter for assessing cracking potential. Moreover, the practicality of Eq. (1) can be enhanced if expressed in terms of RH change, as RH can be obtained either by sensor measurement or simulation based on diffusion theory for various conditions experienced by field concrete members. This requires use of the relationship between shrinkage and concrete RH, which has been established previously as the following[13]

$$\varepsilon = \left[6150\left(1-h\right)\right]\left(1-V_A\right)^n \times 10^{-6} \tag{2}$$

where ε is the shrinkage of the cementitious mixture; h is the RH of the cementitious mixture, expressed as a decimal value; and V_A is the volume fraction of aggregates in the cementitious mixture. Equation (2) was developed based on OPC paste and concretes with a *w/c* of 0.35, 0.4, and 0.45, and the aggregate fraction of concrete was 40%. The n value in Eq. (2) is taken as 1.68 from the previous study,[13] which denotes the aggregate restraining effect on autogenous shrinkage. The value of n can be assumed to be a constant for different aggregate volume contents, according to the study by Pickett[19] for drying shrinkage. As it is known, autogenous shrinkage of a cementitious mixture is mostly determined by capillary pore RH, although other factors such as hydration products, porosity, and unhydrated cement particles are involved. Therefore, the RH-shrinkage relationship is equally applicable to systems with slag cement.

By taking the derivative of Eq. (2) and substituting into Eq. (1), one obtains the following relation for the RH drop rate of a cementitious mixture at the time of cracking

$$\dot{h}_{cr} = -\left(\frac{dh}{dt}\right)_{cr} = \frac{14\left(t_{cr}/24 - 0.1\right)^{-0.87}}{6150\left(1-V_A\right)^{1.68}} \tag{3}$$

The minus sign in Eq. (3) is to ensure that a concrete RH "drop" rate produces a positive value and to be in consistency with the shrinkage rate value.

From Eq. (3), the critical concrete RH drop rate at the time of cracking can be calculated for mixtures containing different aggregate contents, as shown in Fig. 9. The curves indicate the relationship between cracking time (in days) and RH drop rate for mixtures under fully restrained conditions and with V_A = 0, 0.5, 0.65, and 0.75. It can be seen that the cracking tendency decreases with the increase of aggregate content, as indicated by the arrow in Fig. 9, because the cracking time increases for a given RH drop rate. Any curve of RH drop rate versus time that is above the corresponding critical curve, meaning less than the critical RH drop rate value, indicates low cracking potential. For example, under a fully restrained condition, concrete containing 75% aggregate will crack at 3 days or less if the concrete RH drop rate is greater than the critical RH drop rate of 0.01/h. There is no cracking at 3 days or less if the concrete RH drop rate is lower than 0.01/h. Concrete containing less than 50% aggregate is more prone to cracking because, for a given cracking time, the critical concrete RH drop rate is small compared with concrete containing more aggregate. Concrete containing more aggregate requires a greater concrete RH drop rate to crack at a given time, and thus has less cracking tendency.

From Eq. (3), the allowed concrete RH drop rate can be obtained as

$$\dot{h} \le \frac{14\left(t/24 - 0.1\right)^{-0.87}}{6150\left(1-V_A\right)^{1.68}} \tag{4}$$

This expression means that if the rate of RH reduction satisfies Eq. (4), it is expected that the concrete has low cracking potential before time t. Although the aforementioned equations are established from autogenous shrinkage and restrained stress results on sealed-cured specimens, they are applicable to evaluate cracking tendency due to drying shrinkage. Autogenous shrinkage is a consequence of the self-desiccation process and shares the same mechanisms with drying shrinkage. Self-desiccation proceeds with an increasing degree of cement hydration, and the process can be treated as a special type of drying.[20] The difference is that the RH drop due to external drying spans a wide RH range, while self-desiccation is limited to a more narrow RH range (not below 70%). Because the volume of water-filled pores available for hydration to proceed decreases with time in a sealed cement paste, cement hydration slows down drastically when concrete RH drops below approximately 70 to 75%.[18,21] If hydration stops, then further self-desiccation also stops and the RH remains constant. Moreover, autogenous shrinkage develops uniformly in a cementitious mixture and no specimen size effect is involved as compared with drying shrinkage. Therefore, the relationship between RH and shrinkage based on autogenous shrinkage measurements is applicable for characterizing shrinkage due to both self-desiccation and external drying.

To evaluate the cracking potential of concrete by using Eq. (4), the first step is to obtain the concrete RH as a function of time. This can be done either through field RH measurements or numerical simulations. Field measurements can be done by embedding RH sensors in concrete members and monitoring the RH continuously. However, similar to

laboratory measurements, the measured RH values might show variability, with various RH sensors yielding different values. As an example, in this study, the RH development of concrete exposed to different ambient RH conditions was obtained by numerical simulation based on diffusion theory, as stated by the following differential equation

$$\frac{\partial h}{\partial t} = \frac{\partial h_d}{\partial t} + \frac{\partial h_s}{\partial t} = \frac{\partial}{\partial x}\left(D\left(h_d, h_s\right)\frac{\partial h_d}{\partial x}\right) + \frac{\partial h_s}{\partial x} \qquad (5)$$

where $h = h_d + h_s$; h is the concrete RH; h_d is the concrete RH due to external drying; and h_s is the concrete RH due to self-desiccation, which can be obtained either by numerical simulation or measurement on a sealed-cured specimen. In this study, the evolution of h_s was simulated using HYMOSTRUC.[22] The computer program HYMOSTRUC is a microstructural-based model, which can predict RH reduction due to cement hydration and has been proven to be a reliable RH predictor in cementitious mixtures.[23] The input parameters to HYMOSTRUC are *w/cm*, cement composition, and curing temperature. The parameter $D(h_d, h_s)$ in Eq. (5) is the diffusion coefficient for water, which is a function of concrete RH. The widely used equation for $D(h)$ developed by Bažant and Najjar[24] is adopted in this study and is given by Eq. (6)

$$D\left(h\right) = D_1\left(\alpha + \frac{1-\alpha}{1+\left[\left(1-h\right)/1-h_c\right]^{\beta}}\right) \qquad (6)$$

where D_1 is the maximum value of $D(h)$ for $h = 1$; α is the ratio of the minimum value (for $h = 0$) to the maximum value of $D(h)$; h_c is the RH at $D(h) = 0.5D_1$; and β is a parameter that characterizes the extent of the drop of $D(h)$.

The rate of humidity drop due to drying

$$\left(\frac{\partial h_d}{\partial t} \text{ in Eq. (5)}\right)$$

was determined by solving Eq. (7) along with the boundary condition given by Eq. (8)

$$\frac{\partial h_d}{\partial t} = \frac{\partial}{\partial x}\left(D\left(h_d, h_s\right)\frac{\partial h_d}{\partial x}\right) \qquad (7)$$

$$D\left(h\right)\left(\frac{\partial h}{\partial x}\right)_S = S\cdot\left(h_e - h_{sur}\right) \qquad (8)$$

where S is the surface factor for water evaporation; h_e is the ambient RH; and h_{sur} is the RH at the concrete surface. An analytical procedure for solving Eq. (7) and (8) was developed based on the finite difference method,[25] and the algorithm was programmed in MATLAB.

Example

The concrete RH drop rate was computed for different ambient conditions and the cracking potential due to both external drying and self-desiccation were evaluated for

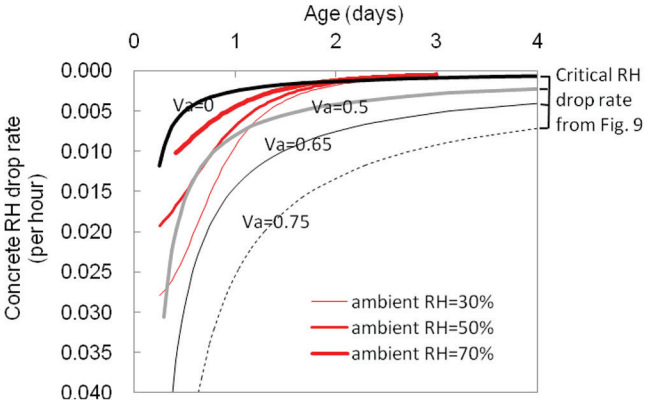

Fig. 10—Calculated concrete RH drop rate at depth of 0.5 cm (0.2 in.) under different ambient RH conditions compared with cracking potential curves from Fig. 9.

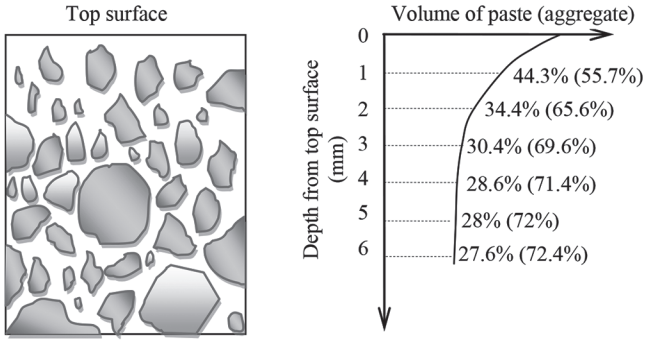

Fig. 11—Variation of aggregate content by volume along depth of concrete (after Kreijger[26]). (Note: 1 mm = 0.0394 in.)

concretes with different aggregate contents (0, 50, 65, and 75%) at *w/c* = 0.4. The cracking potential is evaluated by comparing the computed RH drop rate versus time curve with the critical curves of the RH drop rate at the time of cracking (Fig. 9). For external drying, the top surface of concrete was assumed to be exposed to ambient RH values of 30, 50, and 70%. The parameters in Eq. (6) through (8) were $D_1 = 0.76$ cm^2/day (0.12 in.^{2}/day), $h_c = 0.985$, $\alpha = 0.06$, $\beta = 0.8$, and $S = 0.55$ cm/day (0.085 in.^{2}/day).[24]

Figure 10 shows the calculated concrete RH drop rates at the depth of 0.5 cm (0.2 in.) from the top surface versus age. The curves of the critical RH drop rate established in Fig. 9 are also plotted in Fig. 10. As expected, concrete exposed to a lower RH environment shows a higher RH drop rate. Shrinkage cracking has been traditionally thought to occur only in the near-surface layer or skin of concrete.[26,27] As shown in Fig. 11, the near-surface layer is mostly made of cement paste approximately 0.1 mm (0.004 in.) thick,[26] while the aggregate content increases with distance from the surface. Based on Kreijger's[26] study, the aggregate volume varies from approximately 56% at 1 mm (0.04 in.) to 72% at 5 mm (0.2 in.) from the top surface for a typical concrete mixture. As illustrated in Fig. 10, at a low ambient RH of 30%, concretes with an aggregate content less than 65% are expected to crack within the first day if not appropriately cured. If the ambient RH is 70% or above, there is no cracking potential for concrete with aggregate content in the range from 50 to 75%. However, cracking potential exists for concrete with aggregate content less than 50% if the ambient

RH is 50% or below. This is crucial for the near-surface layer of a concrete member exposed to a dry environment.

CONCLUSIONS

Evaluating the shrinkage cracking potential of a cementitious mixture is an important topic in concrete technology. This study presents a new methodology that focuses on shrinkage rate and RH drop rate in the near-surface layer of concrete members for cracking potential assessment on the basis of experimental measurements and numerical simulations. The major findings of this study are:

1. A restraint rig was used to measure stress development in linear specimens. The induced stresses initially develop as compression and then change to tension in specimens that are restrained starting at very early ages. The stress pattern is consistent with initial thermal expansion followed by autogenous shrinkage development. All paste specimens (w/cm = 0.35, 0.4, and 0.45, with and without slag cement) cracked at ages less than 7 days because of the high rate of shrinkage development. Pastes with a low w/cm show a higher rate of shrinkage, and crack at an earlier time and at a higher strength. Slag cement has the potential of delaying cracking time due to the slower shrinkage rate, especially for high-slag-cement content mixtures, and thus is beneficial in reducing the early-age cracking risk.

2. The occurrence of cracking in cementitious mixtures depends, to a large extent, on the shrinkage rate rather than the shrinkage magnitude. A unique relationship is found to exist between the shrinkage rate and cracking time based on test results on linear specimens for restrained sealed-cured conditions. The critical shrinkage rate at the time of cracking ($\dot{\varepsilon}_{cr}$) decreases rapidly for cracking within the first 2 days and then stabilizes. The smaller the critical shrinkage rate at a given time, the higher the cracking tendency of the cementitious mixture.

3. Due to the difficulties in measuring the free shrinkage and calculating shrinkage stress in actual concrete members, a new methodology has been proposed for evaluating cracking potential. This methodology is based on a relationship between autogenous shrinkage and concrete RH established previously. The new methodology requires knowledge of concrete RH history, which can be obtained through in-place measurements or numerical simulations. It is proposed that the cracking potential is a function of concrete RH drop rate and aggregate content. High aggregate content reduces cracking potential, while high concrete RH drop rate increases cracking potential. Concrete with an aggregate content of 50% or less is highly susceptible to cracking, and thus is crucial for the skin concrete.

4. A diffusion-theory-based analytical procedure can be used to predict the concrete RH drop rate for concrete exposed to different ambient RH conditions.

ACKNOWLEDGMENTS

The authors wish to thank the National Science Foundation of China under Grant No. 51108246 for its support.

REFERENCES

1. Grzybowski, M., and Shah, S. P., "Shrinkage Cracking of Fiber Reinforced Concrete," *ACI Materials Journal*, V. 87, No. 2, Mar.-Apr. 1990, pp. 138-148.

2. Weiss, W. J., and Shah, S. P., "Recent Trends to Reduce Shrinkage Cracking in Concrete Pavements," *Aircraft/Pavement Technology: In the Midst of Change, Sponsors: ASCE, Air Transport Division, Airfield Pavement Committee*, American Society of Civil Engineers, Seattle, WA, 1997, pp. 217-228.

3. Shah, S. P.; Karaguler, M. E.; and Sarigaphuti, M., "Effects of Shrinkage Reducing Admixture on Restrained Shrinkage Cracking of Concrete," *ACI Materials Journal*, V. 89, No. 3, May-June 1992, pp. 289-295.

4. Bentur, A., "Early Age Shrinkage Induced Stresses and Cracking in Cementitious Systems," RILEM Technical Committee 191-EAS, RILEM Publications, 2003, 337 pp.

5. Kovler, K.; Sikuler, J.; and Bentur, A., "Restrained Shrinkage Tests of Fiber Reinforced Concrete Ring Specimens: Effect of Core Thermal Expansion," *Materials and Structures*, V. 26, 1993, pp. 231-237.

6. Paillere, A. M.; Buil, M.; and Serrano, J. J., "Effect of Fiber Addition on the Autogenous Shrinkage of Silica Fume Concrete," *ACI Materials Journal*, V. 86, No. 2, Mar.-Apr. 1989, pp. 139-144.

7. Springenschmid, R.; Gierlinger, E.; and Kernozycki, W., "Thermal Stress in Mass Concrete: A New Testing Method and the Influence of Different Cements," *Proceedings of the 15th International Congress for Large Dams*, Lausanne, Switzerland, 1985, pp. 57-72.

8. Toma, G.; Pigeon, M.; Marchand, J.; Bissonnette, B.; and Barcelo, L., "Early Age Restrained Shrinkage: Stress Build Up and Relaxation," *International Research Seminar: Self-Desiccation and Its Importance in Concrete Technology*, Lund, Sweden, 1999, pp. 61-71.

9. Altoubat, S. A., and Lange, D. A., "Grip-Specimen Interaction in Uniaxial Restrained Test," *Concrete: Material Science to Application—A Tribute to Surendra P. Shah*, SP- 206, P. Balaguru, A. Naaman, and W. Weiss, eds., American Concrete Institute, Farmington Hills, MI, 2002, pp. 189-204.

10. Attiogbe, E. K.; See, H. T.; and Miltenberger, M. A., "Cracking Potential of Concrete under Restrained Shrinkage," *Proceedings, Advances in Cement and Concrete: Volume Changes, Cracking, and Durability, Engineering Conferences International*, Copper Mountain, CO, 2003, pp. 191-200.

11. See, H. T.; Attiogbe, E. K.; and Miltenberger, M. A., "Potential for Restrained Shrinkage Cracking of Concrete and Mortar," *Cement, Concrete and Aggregates*, V. 26, No. 2, 2004, pp. 123-130.

12. ASTM C1581/C1581-09, "Standard Test Method for Determining Age at Cracking and Induced Tensile Stress Characteristics of Mortar and Concrete under Restrained Shrinkage," ASTM International, West Conshohocken, PA, 2009, 7 pp.

13. Wei, Y.; Hansen, W.; Biernacki, J. J.; and Schlangen, E., "Unified Shrinkage Model for Concrete from Autogenous Shrinkage Test on Paste with and without GGBFS," *ACI Materials Journal*, V. 108, No. 1, Jan.-Feb. 2011, pp. 13-20.

14. Bentur, A., and Kovler, K., "Evaluation of Early Age Cracking Characteristics in Cementitious Systems," *Materials and Structures*, V. 36, 2003, pp. 183-190.

15. Springenschmid, R.; Breitenbucher, R.; and Mangold, M., "Development of the Cracking Frame and the Temperature-Stress Testing Machine," *Thermal Cracking in Concrete at Early Ages*, R. Springenschmid, ed., Proceedings of the RILEM Symposium, E&FN Spon, 1994, pp. 137-144.

16. Altoubat, S. A., and Lange, D. A., "Creep Shrinkage and Cracking of Restrained Concrete at Early Age," *ACI Materials Journal*, V. 98, No. 4, July-Aug. 2001, pp. 323-331.

17. See, H. T.; Attiogbe, E. K.; and Miltenberger, M. A., "Shrinkage Cracking Characteristics of Concrete using Ring Specimens," *ACI Materials Journal*, V. 100, No. 3, May-June 2003, pp. 239-245.

18. Powers, T. C., and Brownyard, T. L., "Studies of the Physical Properties of Hardened Portland Cement Paste," *ACI Journal*, V. 43, No. 9, Sept. 1947, pp. 101-132.

19. Pickett, G., "Effect of Aggregate on Shrinkage of Concrete and Hypothesis Concerning Shrinkage," *ACI Journal*, V. 56, No. 1, Jan. 1956, pp. 581-590.

20. Grasley, Z. C., "Measuring and Modeling the Time-Dependent Response of Cementitious Materials to Internal Stresses," PhD thesis, University of Illinois at Urbana-Champaign, Urbana, IL, 2006, 216 pp.

21. Jensen, O. M., "Thermodynamic Limitation of Self-Desiccation," *Cement and Concrete Research*, V. 25, No. 1, 1995, pp. 157-164.

22. Van Breugel, K., "Simulation of Hydration and Formation of Structure in Hardening Cement-Based Materials," PhD thesis, Delft University of Technology, Delft, the Netherlands, 1991, 295 pp.

23. Koenders, E. A. B., "Simulation of Volume Changes in Hardening Cement-Based Materials," PhD thesis, Delft University of Technology, Delft, the Netherlands, 1997, 171 pp.

24. Bažant, Z. P., and Najjar, L. J., "Nonlinear Water Diffusion in Nonsaturated Concrete," *Materials and Structures*, V. 5, 1972, pp. 1-18.

25. Crank, J., *The Mathematics of Diffusion*, second edition, Clarendon Press, Oxford, UK, 1975, 424 pp.

26. Kreijger, P. C., "The Skin of Concrete—Composition and Properties," *Materials and Structures*, V. 17, No. 100, 1984, pp. 275-283.

27. Pigeon, M.; Marchand, J.; and Pleau, R., "Frost Resistant Concrete," *Construction & Building Materials*, V. 10, No. 5, 1996, pp. 339-348.